GEM TN-92-210

Preliminary Beam Test Results of the GEM Copper/Scintillating Fiber Hadron Calorimeter Prototype

R. Carey, J. Miller, L. Sulak, B. Worstell - Boston University
H. Paar - University of California, San Diego
B. Moore, J. Reidy - University of Mississippi
R. Kroeger - University of Tennessee

October 7, 1992

Abstract:

In July 1992 the SSCintCAL collaboration tested 7 prototype projective hadron calorimeter towers (total mass - 5T) in the BNL A3 test beam. Each tower was constructed with scintillating fibers embedded between cooper laminations. We obtained a fitted energy resolution of 91%/ sqrt (E) for 10 GeV pions, before any corrections for lateral shower containment. We have also not corrected fro fiber attenuation effects, which were significant with our unmirrored (due to time constraints) fibers; this effect is much smaller for jets than for single hadrons. Pions exhibit uniform response when scanned across boundaries between modules and when scanned through a range of incident angles with respect to the fibers. Our measured e/π ratio is $1.08 \pm .02$ before leakage corrections, for pion energies between 10 and 20 Gev. For muons, we observed Landau distributions well-resolved from pedestals for an incident angle of 1.5 degrees with respect to horizontal planes of fibers and 0 degrees with respect to vertical planes of fibers.

GEM-TN-92-210

Preliminary Beam Test Results for the GEM Copper/Scintillating Fiber Hadron Calorimeter Prototype

R. Carey, J. Miller, L. Sulak, B. Worstell
Boston University
H. Paar
University of California, San Diego
B. Moore, J. Reidy
University of Mississippi
R. Kroeger
University of Tennessee

Abstract

In July 1992 the SSCintCAL collaboration tested 7 prototype projective hadron calorimeter towers (total mass = 5T) in the BNL A3 test beam. Each tower was constructed with scintillating fibers embedded between copper laminations. We obtained a fitted energy resolution of $91\%/\sqrt{E}$ for 10 GeV pions, before any corrections for lateral shower containment. We have also not corrected for fiber attenuation effects, which were significant with our unmirrored (due to time constraints) fibers; this effect is much smaller for jets than for single handrons. Pions exhibited uniform response when scanned across boundaries between modules and when scanned through a range of incident angles with respect to the fibers. Our measured e/π ratio is $1.08 \pm .02$ before leakage corrections, for pion energies between 10 and 20 GeV. For muons, we observed Landau distributions well-resolved from pedestals for an incident angle of 1.5 degrees with respect to horizontal planes of fibers and 0 degrees with respect to vertical planes of fibers.

October 7, 1992

1 Overview

In July 1992 the SSCintCAL collaboration tested 7 prototype projective hadron calorimeter towers, each constructed with scintillating fibers embedded between copper laminations. The entire collaboration contributed to the construction and testing of this device, and the author list for this note is only intended to indicate those directly involved in this particular study of the collected data. The total mass of hadron calorimeter prototype constructed and tested in the BNL beam was 5400 kg, supported by a test stand with 4 degrees of freedom. Tests were carried out with incident electrons, pions, and muons with momenta between 1 and 20 GeV/c; the bulk of the data was for pions with 15 GeV or 20 GeV total energy. Calibrations were performed with electrons incident on each of the towers individually, at 10 and 15 GeV. All data was collected with ADCs using a gate width of 100ns.

The fiber packing fraction was 2.25%, which was partially dictated by readily available copper sheet and tubing (we had intended 3%). The nuclear interaction length within these towers was 15.1 cm and the radiation length 1.45 cm. The spacing between fibers was 8.0 mm (square lattice), and the effective Moliere radius 11.6 mm. Each projective tower was 15cm x 15 cm on the front face, 31cm x 31cm on the back face, 160 cm long, and had all fibers parallel to the tower's axis of symmetry. All fibers within a given tower were gathered in a bundle at the larger tower end, then optically mated to a hexagonal light mixer and read out with a single 3" green-enhanced photomultiplier. Because of the projective geometry, most fibers were shorter than 160 cm and terminated at the tapered sides of the module.

The fibers used were green 3HF radiation-hard fibers from Bicron, of 1.35 mm diameter (cladding thickness=50 microns). Due to time limitations, these fibers were not measured or sorted in any way, but were inserted into calorimeter modules just as received from the vendor. Due to early concerns to maximize light yield (these concerns proved unfounded), no filtering was introduced into the optical readout chain; such filtering can remove short attenuation-length components in the scintillation light, resulting from self-absorption at short wavelengths as discussed below. The fiber effective attenuation length is 4 meters after the first 1 meter, but is significantly shorter within the first meter because of self-absorption. Attenuation lengths of greater than 8 meters have been achieved by the SPACAL group with aluminized upstream fiber ends, but we had no time to mirror our fibers

before our beam tests.

In analyzing the test beam results, we have compared our observations with Monte Carlo prediction from both GEANT and CALOR89. We used two GEANT simulations, one for electrons alone and one for pions, electrons, and muons. For electrons, whose showers are completely contained by a single module, we approximated our modules with a regular square lattice geometry: a copper matrix with .3175 cm grooves cut at .793 mm intervals. Inside each groove is a copper tube with .3175 cm outer and .15875 cm inner diameter and in the tube is a 1.35 mm fiber. A 40 micron cladding layer was considered dead material. For the pions, we constructed a stack of hadronic calorimeter modules, whose dimensions and placement were those in the test beam, but whose internal structure was simpler: fibers inside a copper matrix, but with the same sampling granularity as above. Cutoffs were set at 10 keV for photons and 100 keV for electrons. Typical simulation times were of order 45 CPU-seconds per event on a Silicon Graphics Indigo RISC workstation (13 mips) for a 15 GeV pion. We used the GHEISHA hadronic shower simulation with GEANT; we have since become aware of RD1 (SPACAL) GEANT studies with FLUKA which more nearly reproduce hadronic test beam data for fiber calorimeters.

A series of simulations of the SSCintCal fiber calorimeter is also in progress using CALOR89. The CALOR89 program incorporates EGS for electromagnetic processes, MORSE for low-energy neutron production and transport, and SPECT for the transport of higher-energy hadrons; it also incorporates Birk's suppression of scintillation light yield for heavily-ionizing charged particles. The combinatorial geometry package was used to simulate electron showers in one of the SSCintCal towers. For pion showers, the seven-tower structure used in the beam was approximated by one large projective tower with a mass equal to that of all seven towers, and with the same depth. The fibers were incorporated into the geometry with a spacing of 7.95 mm between the centers of the fibers, an active diameter of 1.25 mm for the fibers, and a 0.05 mm plastic cladding around the active fiber. The simulations were carried out on the DECfarm at the University of Mississippi using 18 DECstation 5000/Model 200's. A few runs for incident electrons were also carried out Suns on the PDSF facility at the SSC Laboratory. The CALOR89 runs for incident pions at 5 GeV required 30-35 CPU-minutes per event, with energy cutoffs of 100 keV for photons and 1 MeV for electrons.

2 Results with Pions

Figure 1 illustrates the measured response to 5, 10, 15, and 20 GeV pions. At each energy the response is not gaussian, with some asymmetry and high-energy tail. We believe this is due both to attenuation effects in our unmirrored fibers, and to lateral shower leakage. These effects will be discussed in more detail below. Figure 2(a) shows the $e/over\pi$ ratio as a function of energy, where no corrections have been made for leakage with the pion showers or for slightly increased attenuation with electron showers relative to pions. Figure 2(b) shows the measured resolution (both sigma/mean and fitted sigma/mean) and our $\frac{90\%}{\sqrt{E}}$ specification for comparison. Because of the non-gaussian response, the unfitted resolution is significantly worse than the fitted resolution.

The lateral shower spread for a Cu/SF hadron calorimeter is somewhat wider than for a Pb/SF hadron calorimeter, because of the greater importance of neutrons to the detector response for the former device. In a lead device electromagnetic response suppression is much greater than for a copper device, and the hadronic response must subsequently be boosted more to achieve compensation with a copper device; this is the reason why the packing fraction must be so much lower to achieve compensation with a copper/fiber calorimeter. Electromagnetic suppression arises because the cross section for ionization is proportional to Z, while pair production goes like Z^2 and the photoelectric effect goes like Z^5. Consequently, shower gammas produce low energy electrons preferentially in the high-Z absorber, where they range out. Lateral neutron leakage from our test stack gives an artificially high $\frac{e}{\pi}$ ratio, by suppressing the average response to hadronic activity. Hadronic showers with a large electromagnetic component (early π^0 production) are more contained, and are not suppressed; this combination of mean suppression and stochastic fluctuations for a fraction of unsuppressed showers gives an asymmetric response function.

There is a second effect which contributes to our non-gaussian response. As noted earlier, our fibers were neither selected, filtered, nor mirrored. As a result, longitudinal shower fluctuations result in a high-energy tail, through enhanced light collection for late-developing showers. The light yield from our fibers fits the sum of two exponentials, one with a 5 meter attenuation length (no self-absorption) and a second with a 40 centimeter attenuation length (self-absorption). Because of self-absorption by 3HF

wavelength-shifter (Stokes-shift overlap), short wavelength light has a significantly shorter attenuation length than does longer-wavelength light. This results in an effective fiber attenuation length which decreases markedly for distances between the light production and light collection points of less than 50 centimeters along a fiber; filtering out short-wavelength light can eliminate this effect by removing Stokes-shift overlap. In addition, SPACAL has reported that mirroring fiber ends results in an effective attenuation length of more than 8 meters, plus an 80% increase in overall light yield.

Figure 3(a) shows measured light yield vs excitation position for our 3HF fibers, both before and after irradiation with a dose of 3.6 MRad delivered at a rate of 24 krad/hour. The decreased attenuation for deep showers is readily apparent, resulting in a factor of 2 increase in light yield from the front to the back of the tower. Figure 3(b) shows the sum of two exponentials which best fit our data, and which was used in our simulations of attenuation effects. As noted above, these effects can be eliminated through filtering, mirroring, or both. Figure 4 shows a GEANT Monte Carlo prediction of 10 GeV pion showers with attenuation effects taken into account.

We are still evaluating the relative contributions of lateral shower leakage and of attenuation effects with the help of Monte Carlo simulations. Note that both effects would be eliminated in the final calorimeter; summing across many towers for jets would eliminate lateral leakage, while mirroring fiber ends would greatly diminish attenuation effects. As has been pointed out by the SPACAL group, Gauss's central limit theorem applies to a hadron calorimeter (with a slightly asymmetric response to single hadrons) responding to jets. Independent fluctuations of the hadron showers within the jet combine to give a gaussian response to jets; this was demonstrated by SPACAL for "mini-jets" produced by interactions in an upstream hadronic target.

Figure 5 illustrates the measured correlation between the total response and the fraction of the hadron shower energy which is collected within the central tower only. Large signals correlate with a large fraction of the shower energy in the central tower. This is consistent with hadronic showers with a large electromagnetic fraction being better contained, and thus giving a higher overall response. It is also consistent with attenuation effects, since deep showers typically have a larger fraction of their energy deposited in the central tower. Figure 6 indicates that the high-energy tail is NOT due to an angle effect like that for electrons (see below); pions incident nearly parallel

to the fiber axes do not have more high-energy tail.

Figure 7 shows the measured uniformity of detector response, and also shows that shower leakage is not more than a few % for 20 GeV pions. Figure 7(a) shows the response to pions scanning horizontally across the boundaries between towers; these boundaries are at -8cm and +8cm (this is the central layer containing 3 modules). There is no evidence of reduced response at the module boundaries, and leakage is small as long as the pion beam is incident on the central tower. Electrons are a more sensitive probe of local response, and Figure 7(b) shows data from a horizontal scan across module boundaries at 0 (this is the top layer containing 2 modules). The system response to electrons actually increases by almost 10% at the module boundary, in contrast to SPACAL's experience with projective modules. This may be explained by our "staircase" construction, with which we intentionally oversample near module boundaries. By slightly shortening fibers/tubes at module boundaries we can make this transition completely uniform.

The response of the scintillator is fast, and although we used 100 ns wide gates the pulse arrival was typically 20ns into the gate. Due to beam time constraints, we were unable to measure the dependence of $e/over\pi$ on gate width, but we were able to record several pion pulse waveforms with a high-bandwidth digital oscilloscope. Figure 8 shows a typical pion pulse (this signal is only from the central tower), with a risetime of 4ns (10% - 90%) and a FWHM of 10.5ns. Some of the response at late times seen on the pulse is due to dispersion in the delay cables, which were 400ns of RG-58.

Figure 9 illustrates CALOR89 predictions for electromagnetic and hadronic resolution and $e/over\pi$ for our calorimeter stack. The electrons were all produced at a single incident position, so there are no high-energy tails from the incident position effect ("channelling") described below. The predicted resolution for electrons is $\frac{70\%}{/sqrtE}$, and for pions is $\frac{90\%}{\sqrt{E}}$. The predicted e/h is 1.20 at 5 GeV and 1.10 at 10 GeV. We continue to study the effects of cut-offs and geometric simplifications on our CALOR89 results.

We have also tried "tuning" GEANT to reproduce our test beam data. The overall fraction of incident energy deposited in fibers is first determined for electrons. For pions, we then separately collect "electromagnetic" and "hadronic" energy deposition within a hadron shower. GEANT attempts to simulate compensation phenomena such as recoil protons from neutrons, but it in fact overestimates the fiber energy deposition from the hadronic part of a shower. We tune GEANT's e/h so as to reproduce the $e/over\pi$ which

we measured in the test beam at 15 GeV. Note that "untuned" GEANT energy deposition in fibers predicts an $e/over\pi$ for our geometry at 15 GeV of 0.91, where we measured $e/over\pi = 1.08$. The response distribution for the resulting simulation and for data are compared in Figure 10. Both exhibit an asymmetric response. GEANT predicts that a larger tower with less leakage would have had a substantially more Gaussian response, as indicated in figure 11; figure 11(b) shows that the remaining high-energy tail corresponds to showers with a small EM fraction. This GEANT study also indicates that the $e/over\pi$ ratio is underestimated because of the leakage, and by summing over more towers we would be overcompensated ($e/over\pi = 0.97$).

3 Results with Electrons

All modules were calibrated with 10 and 15 GeV electrons at large incident angles, and these calibrations agreed to within 2% over a week of running. Light yields from our prototype modules were evaluated by two independent methods. First, we calibrated PMT gains with LEDs (for constant illumination the fluctuations in signal collection reflect photostatistics) and applied this calibration to calorimeter signals. Second, we introduced neutral density filters between the calorimeter and the photomultiplier and measured the increase in width of the calorimeter's gaussian response to electrons. Both methods agreed in giving 60 PEs/GeV for electrons; this exceeds our system specification of 40 PEs/GeV. Note that this yield would increase with mirrored fibers or with increased packing fraction.

Studies of the response of the calorimeter to electrons over a range of energies and angles of incidence showed qualitative agreement with the results from SPACAL. Figure 12(a) show the response to 15 GeV electrons at an incident angle of 3.5 degree in yaw 5.1 degrees in pitch. The high energy tail arises due to channeling and its relative size depends stongly on the incident angle. Figure 12(b) shows for comparison the pulseheight spectrum at the same energy but at a pitch of 10.1 degrees - the high energy tail is largely eliminated.

GEANT simulations confirm the position and angular dependence of the high energy tail. The effects were slightly exaggerated in the Monte Carlo simulations because a switch for "Gaussian" rather than "Moliere" response was mistakenly left set in the GEANT simulations. Figure 13 shows the

Monte Carlo calorimeter response for 15 GeV incident electrons striking a 1mm wide vertical slice of calorimeter which passes through a fiber. As the incident position changes in y (vertical sweep) the response increases dramatically in the vicinity of the fiber. Therefore, at steep incident angles the calorimeter response is large when the electron is incident on or near the fiber and much less away from the fiber.

At somewhat larger incident angles, there is still a strong correlation between the incident position and the response, although it does not correspond to channeling in the usual sense. For a pitch of 3.5 and yaw of 10.1 the direction cosine in y is almost exactly three times that in the x direction. Therefore if a particle comes in along the line $y = 3x$, (where it is assumed that a fiber is centered at the origin), its path will take it through the plane of fibers $y = 3x$ until it is scattered. The same is true for particles which come in along the lines $y = 3x/plmilatticespacing * \sin\tan^{-1}(1/3)$.

The high energy tails we see in the electron Monte Carlo data are not expected to be important in the GEM environment since showering in electromagnetic calorimeter will smear out the incident energy over a range of incident angles and positions. Figure 14 shows GEANT results for the resolution on energy leaking through 20 radiation lengths of lead from 100 GeV electrons at normal incidence. (This simulation was inspired by the question of what the resolution on the energy leakage from a 400 GeV Z' decay-electron incident on a 25 radiation length EM calorimeter might be). The quantity plotted in Figure 14(d) is the deviation from its mean value of the ratio of energy in the fiber to the total energy leaking into the hadron calorimeter, with this deviation normalized by the total leakage energy, in GeV. The leakage resolution is $45\%/over\sqrt{E}$ and there is no sign of a high energy tail.

4 Results with Muons

Due to beam time constraints, we did very little running with a dedicated muon trigger. Figure 15 shows the calorimeter response to one such dedicated run, with muons incident at 1.5 degrees in pitch and 0 degrees in yaw. This meant that the muons effectively saw vertical sheets of fibers. Despite the small angle (and zero angle in the other direction) the response to muons is clearly separated from pedestal. In addition, there is some background present from pion showers in the calorimeter producing punch-through muons

for the trigger. In the GEM detector configuration we will maintain at least 2 degrees in both pitch and yaw between fiber axes and muons, by aligning fibers with projective module boundaries and through "pinwheel" pointing of nearly projective towers.

5 Conclusions

Our test device met the GEM hadron calorimeter design specifications. The measured e/h ratio was ≈ 1.15 before lateral leakage corrections, and may in fact be less than 1 after these corrections. Our asymmetric test beam response to pions was due to lateral leakage and fiber attenuation effects which will not be present in the final GEM device. Our measured (fitted) hadronic resolution of $\frac{91\%}{\sqrt{E}}$ already meets the GEM specifications, and will be significantly improved by decreasing attenuation with mirrors and by summing across more calorimeter towers. The response to electromagnetic leakage of $\frac{45\%}{\sqrt{E}}$ also exceeds the GEM specification. We have therefore demonstrated a fast, compensating Copper/scintillating fiber hadron calorimeter suitable for GEM.

Figure 1

Test Beam Data

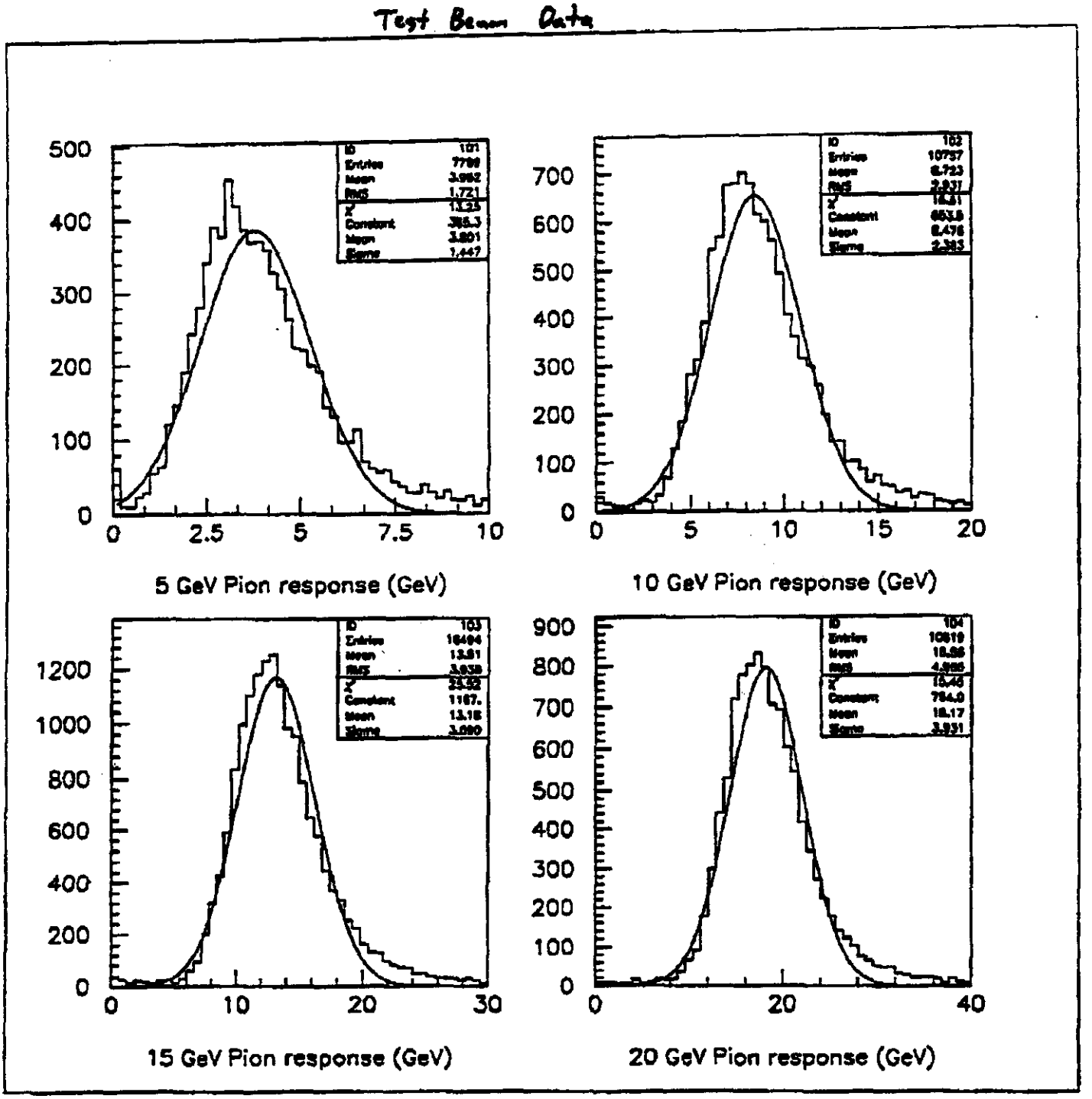

Figure 2

Test Beam Data

Uncorrected E/Pi

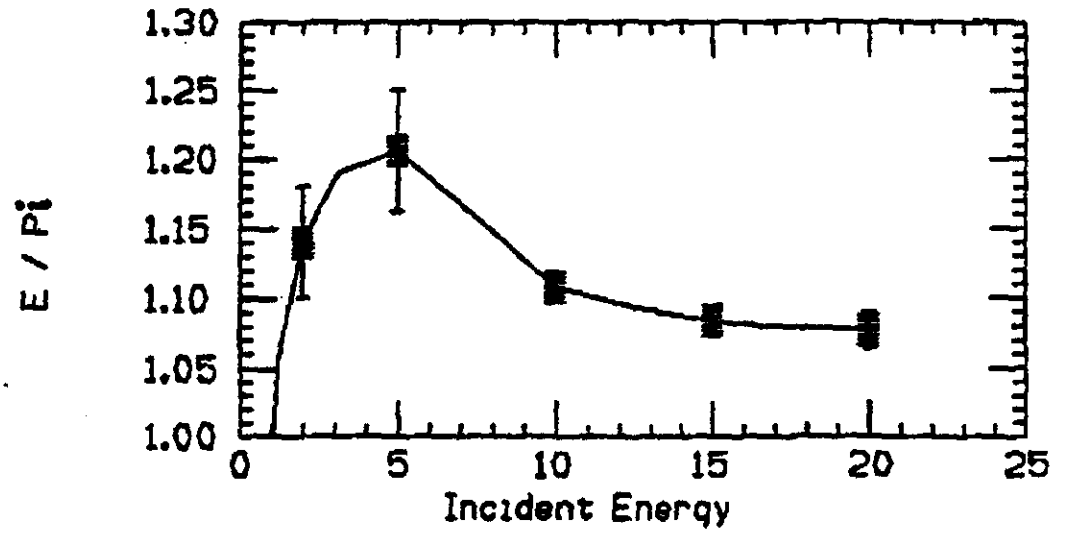

Hadronic Resolution - No Corrections

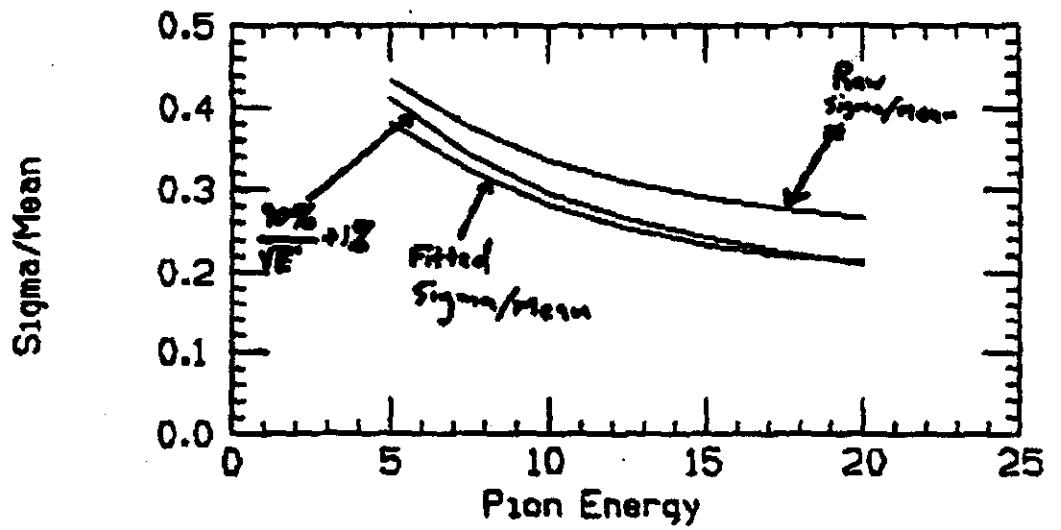

Figure 3

Bench Test Data

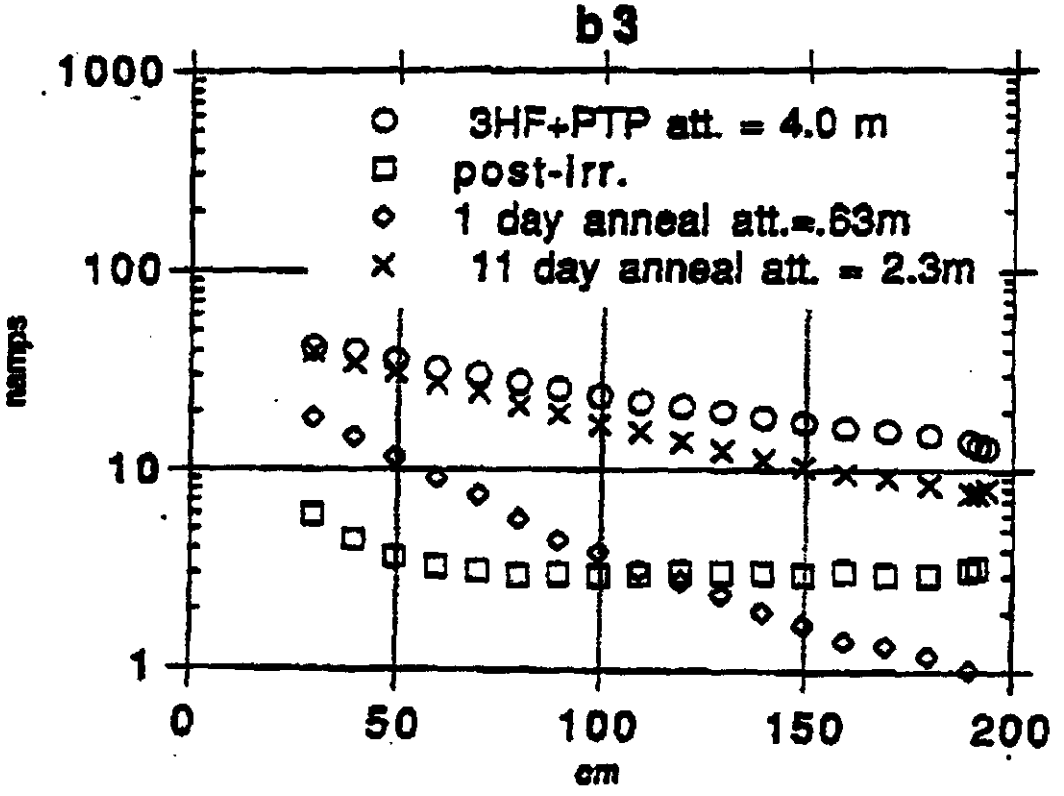

Fit to Bench Test Data

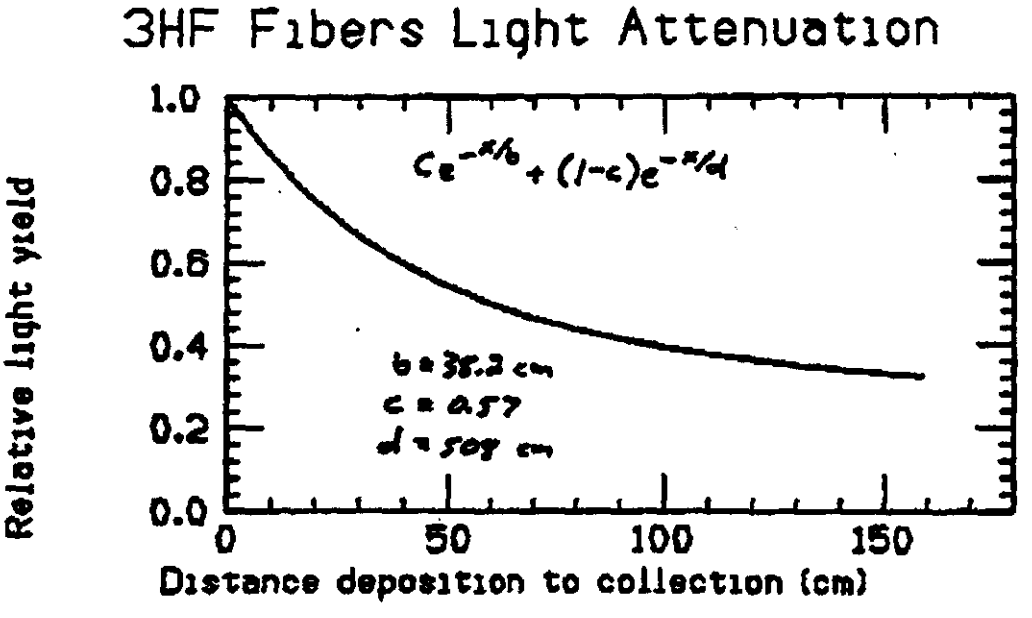

Figure 4

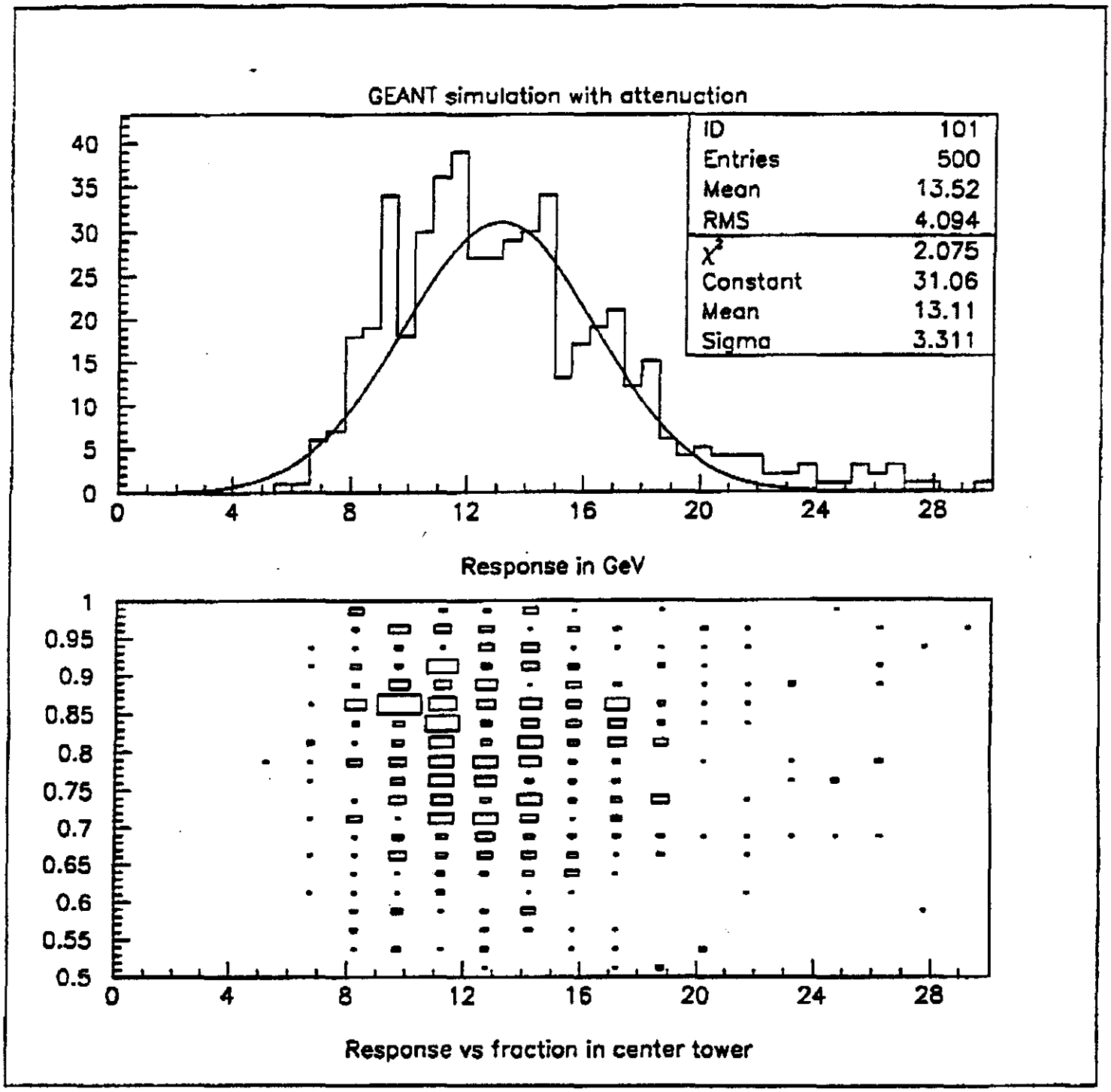
GEANT simulation with attenuation
ID 101
Entries 500
Mean 13.52
RMS 4.094
χ² 2.075
Constant 31.06
Mean 13.11
Sigma 3.311
Response in GeV
Response vs fraction in center tower

Figure 5

Test Beam Data

20 GeV Pion Data

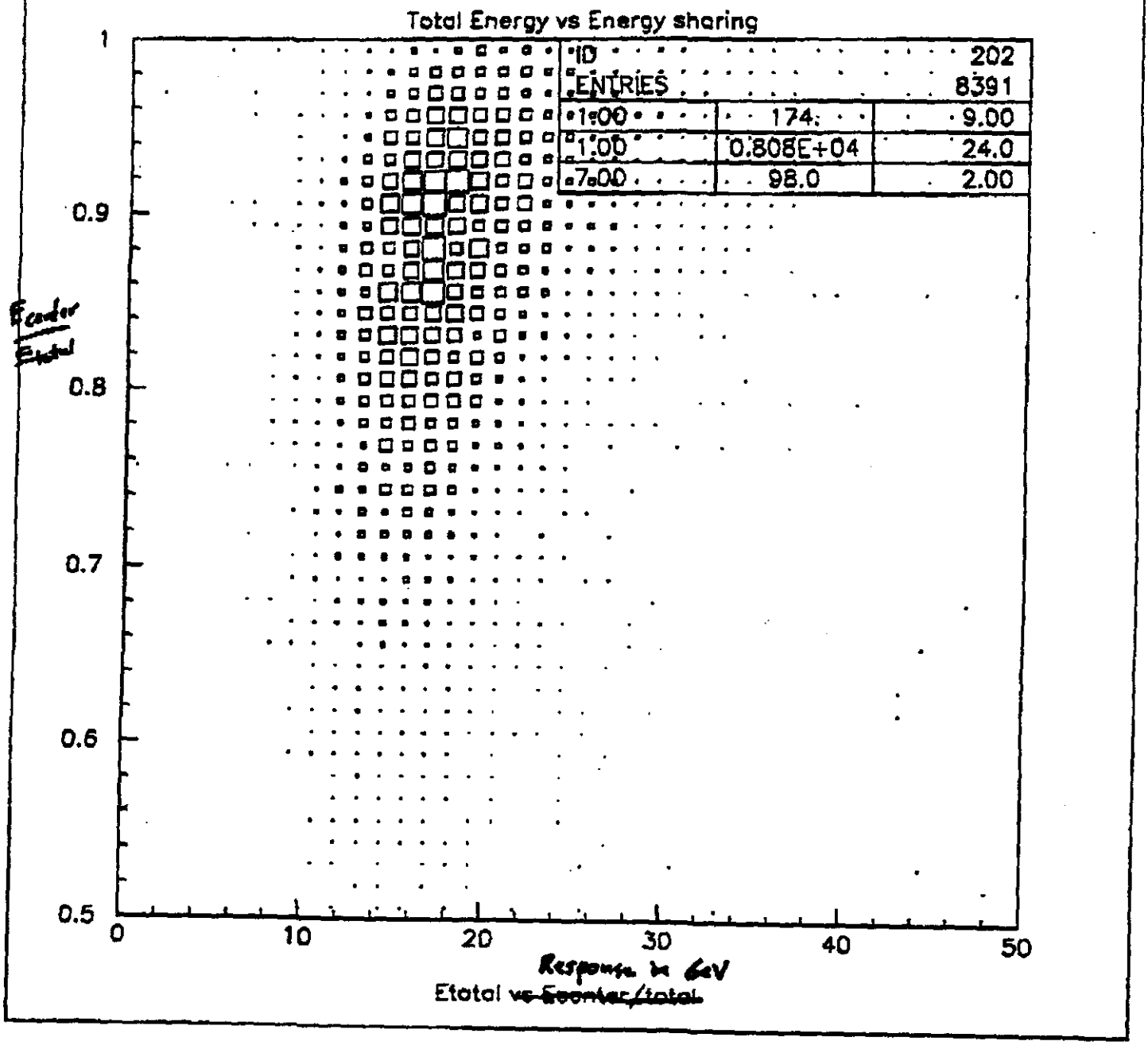

Figure 6

Test Beam Data

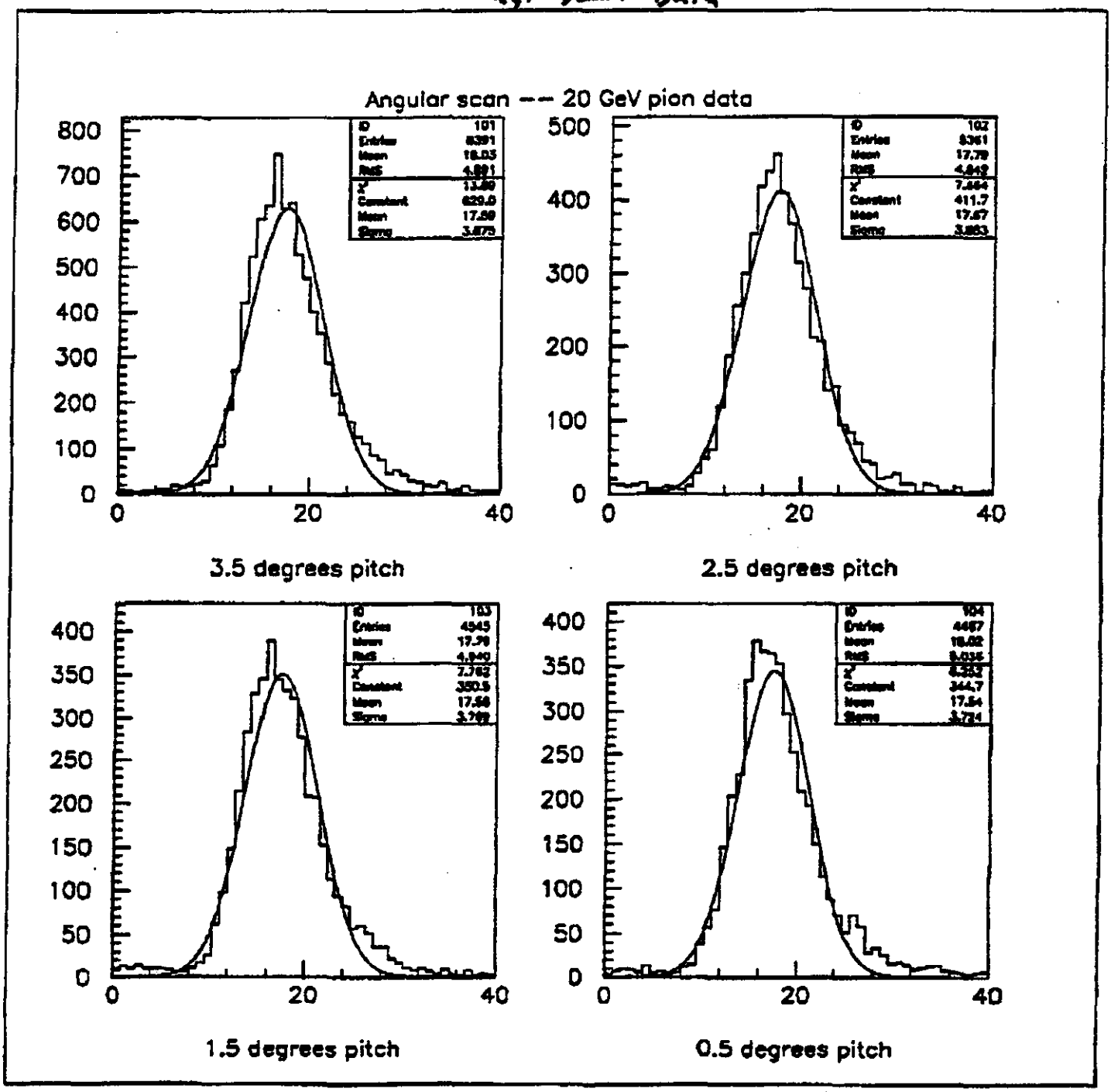

Figure 7

Test Beam Data

Response to 20 GeV pions vs. Incident position

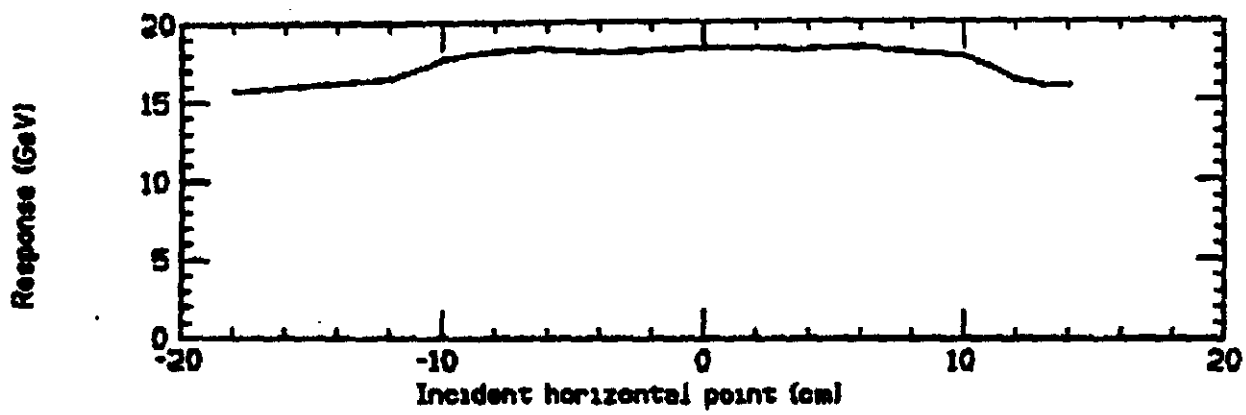

Response to 10 GeV Electrons vs. Incident position

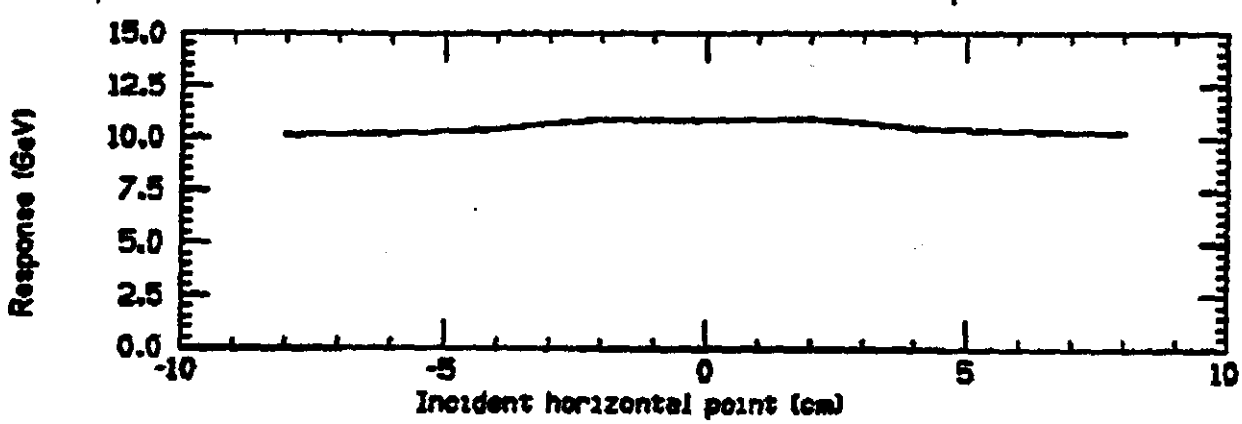

Test Beam Data

Figure 8

15 GeV π^-

Scintillator

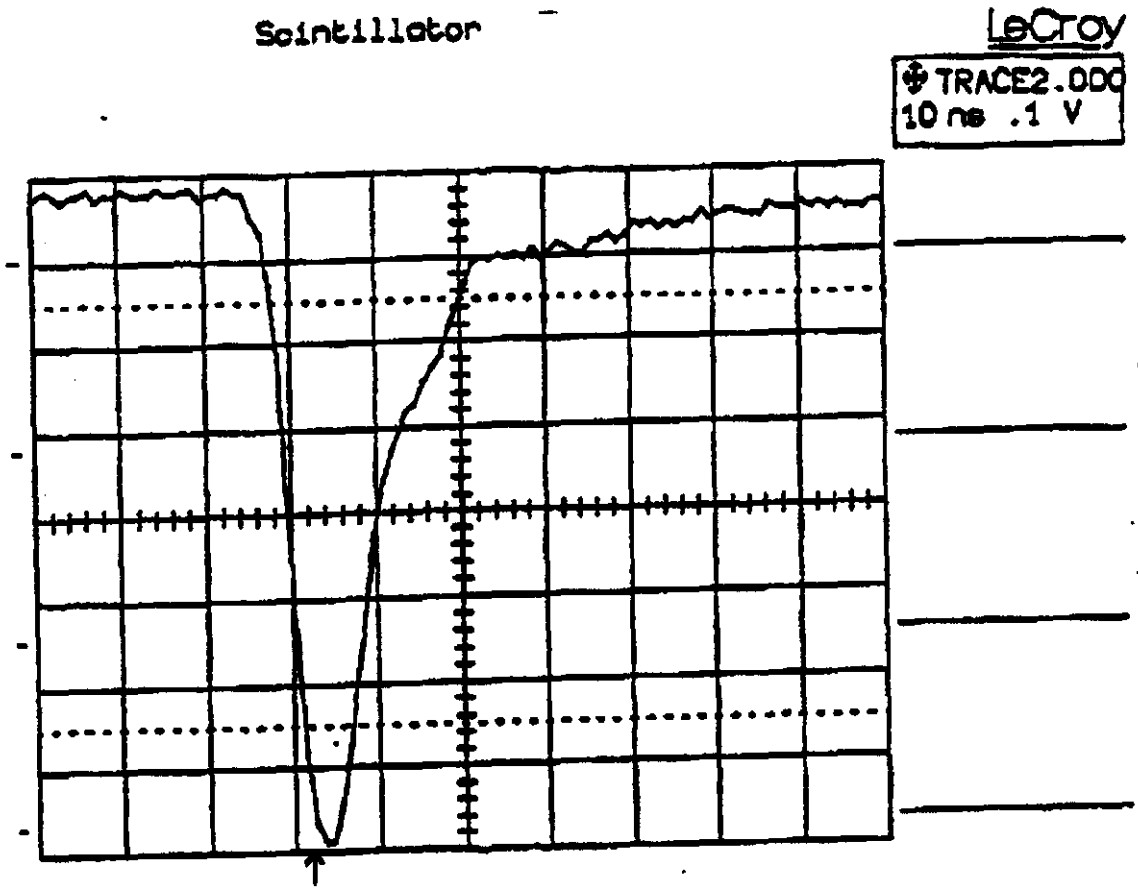

Scintillator

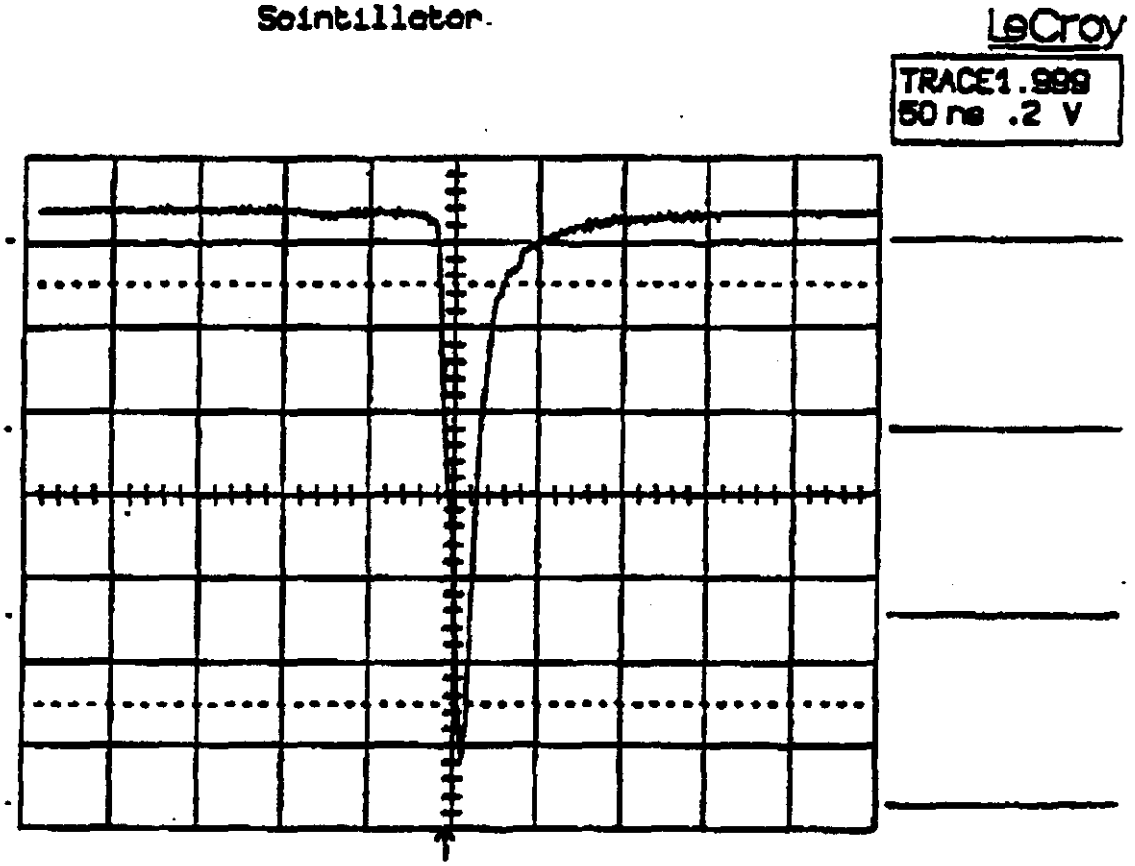

Figure 9

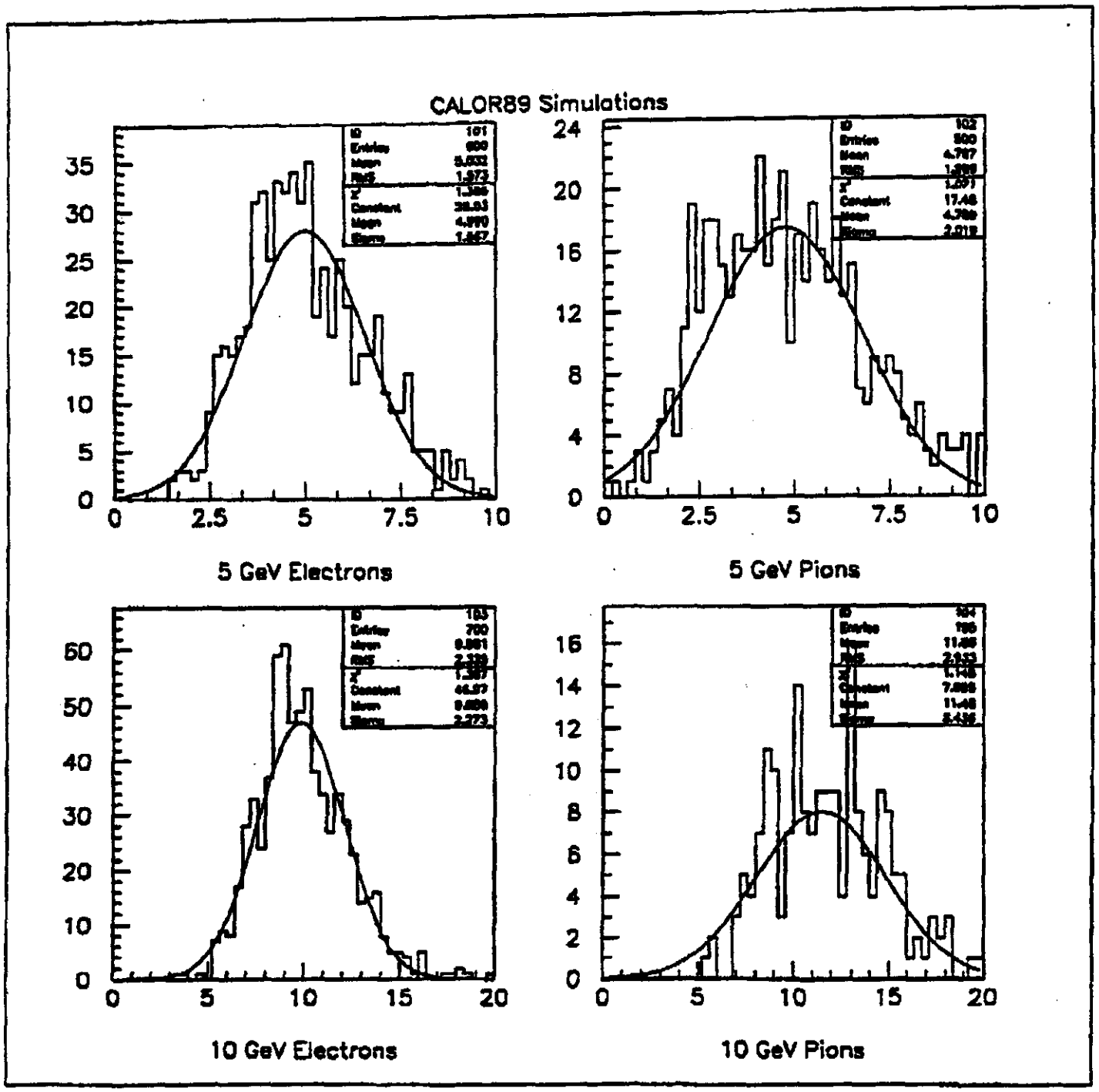
CALOR89 Simulations
5 GeV Electrons
5 GeV Pions
10 GeV Electrons
10 GeV Pions

Figure 10

'Tuned' GEANT Simulations

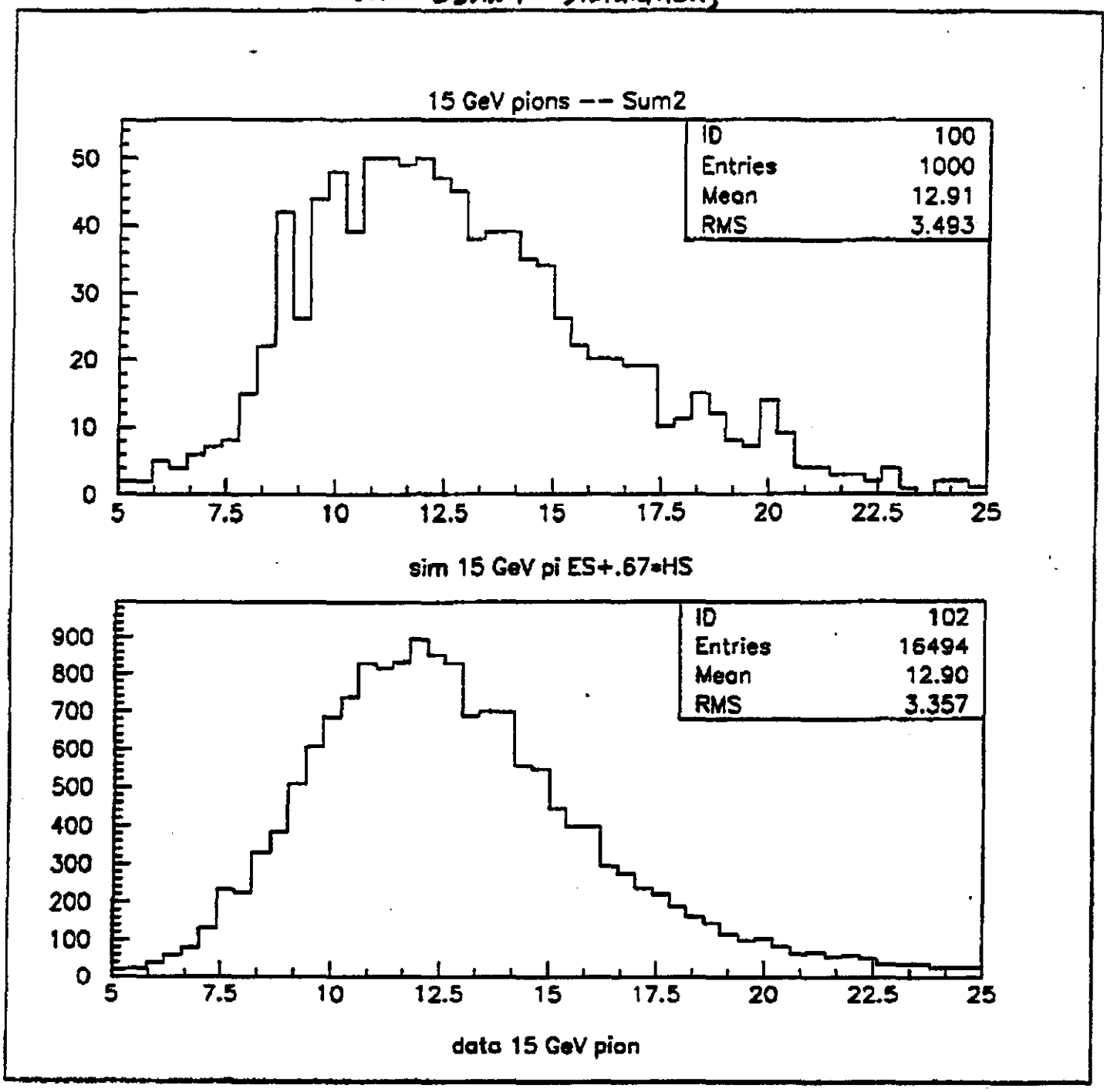

Figure 11

'Tuned' GEANT Simulation

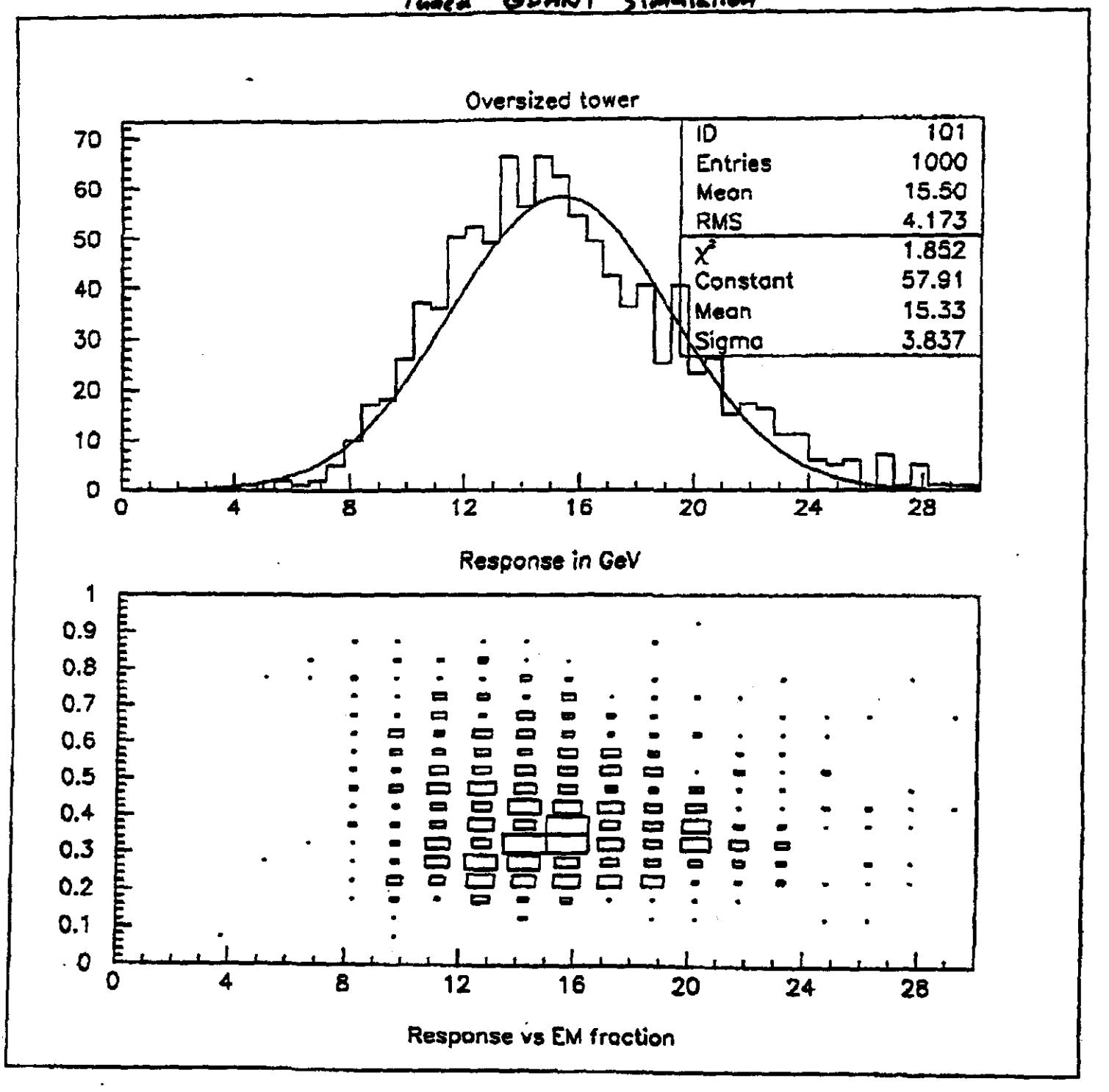

Figure 12

Test Beam Data

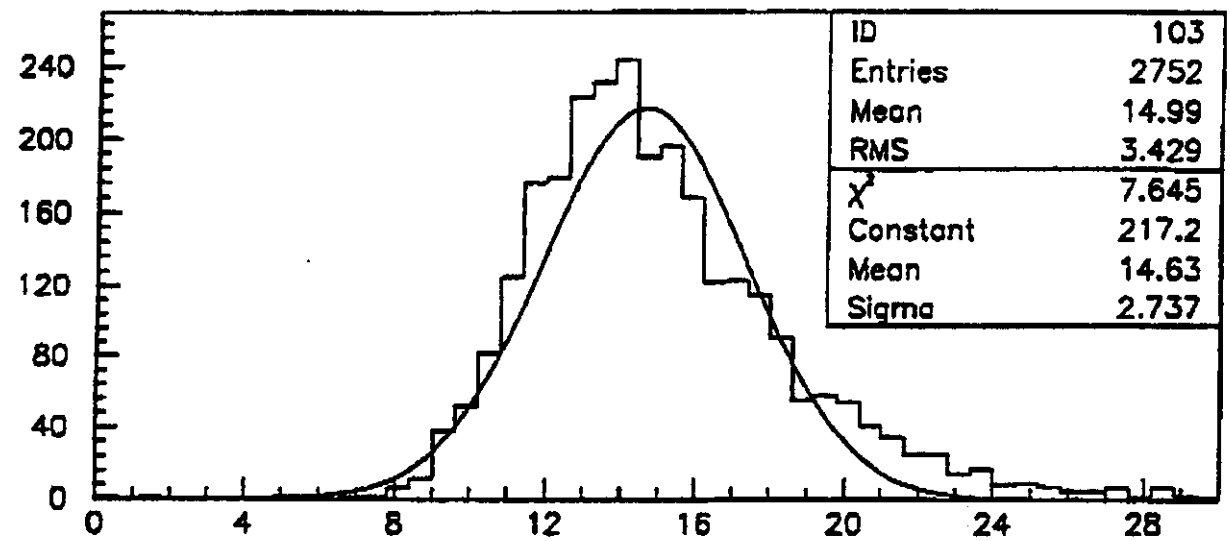

15 GeV electron – pitch 5.1 yaw 3.5

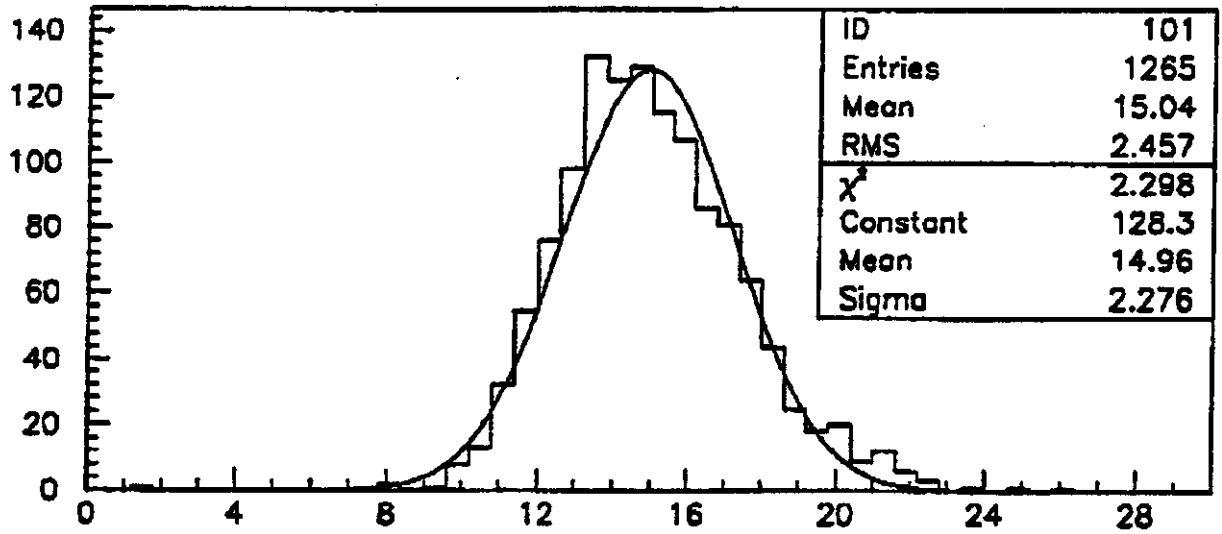

15 GeV electron – pitch 10.1 yaw 3.5

Figure 13

GEANT 1mm vertical slice of calorimeter

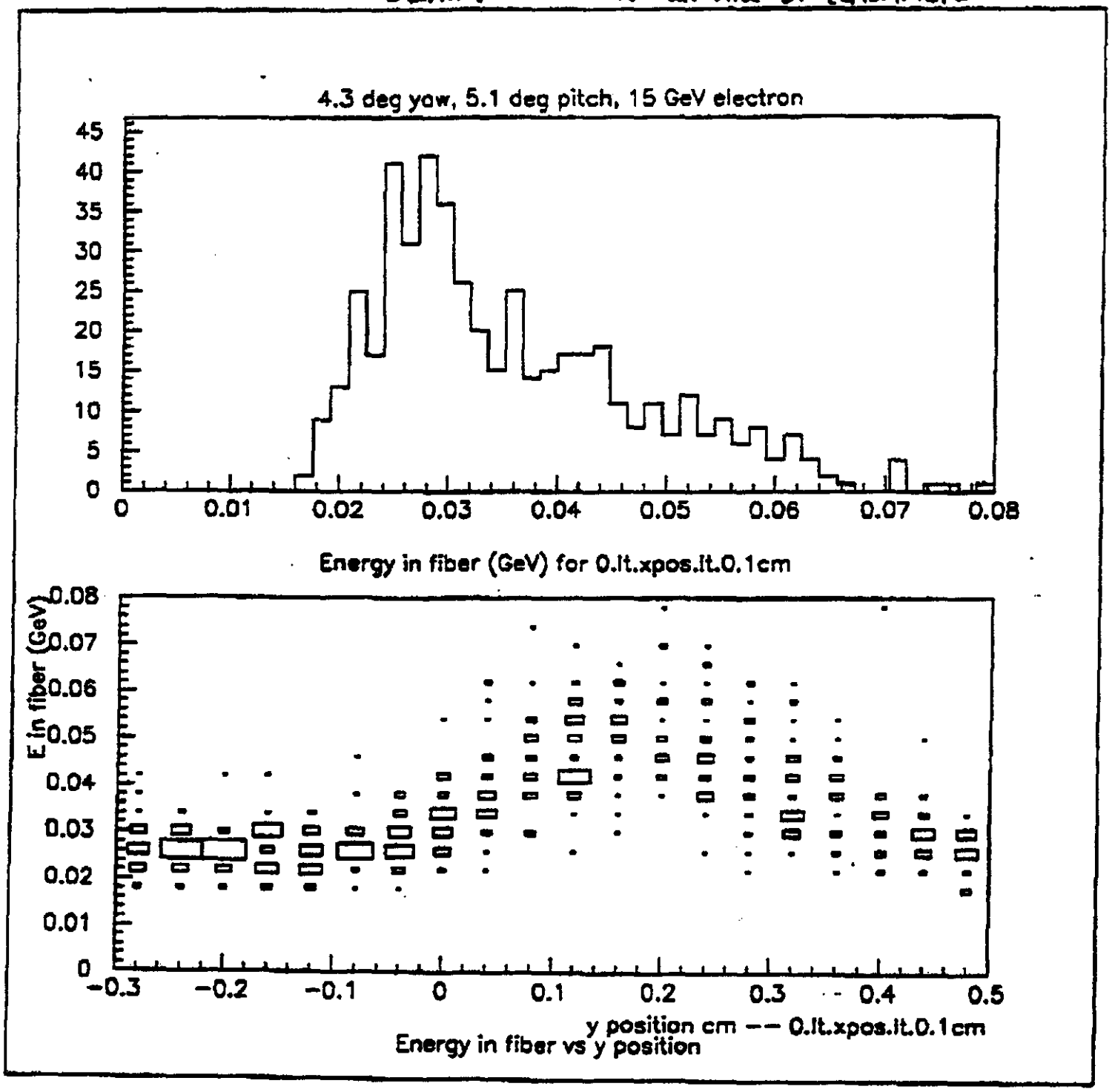

Figure 14

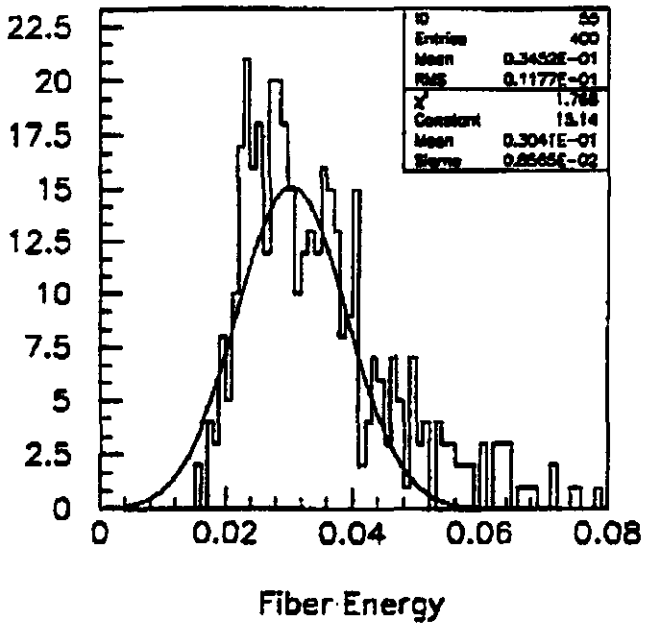
22.5
20
17.5
15
12.5
10
7.5
5
2.5
0
0
0.02
0.04
0.06
0.08
Fiber Energy

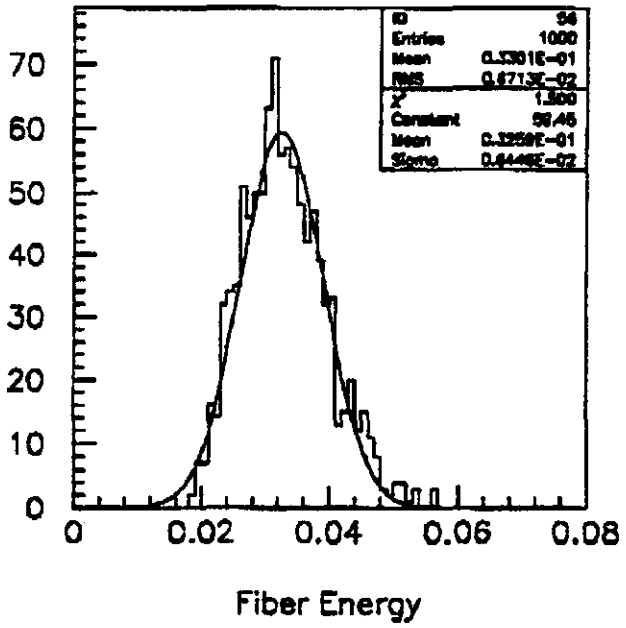
70
60
50
40
30
20
10
0
0
0.02
0.04
0.06
0.08
Fiber Energy

Figure 15

GEANT Simulation

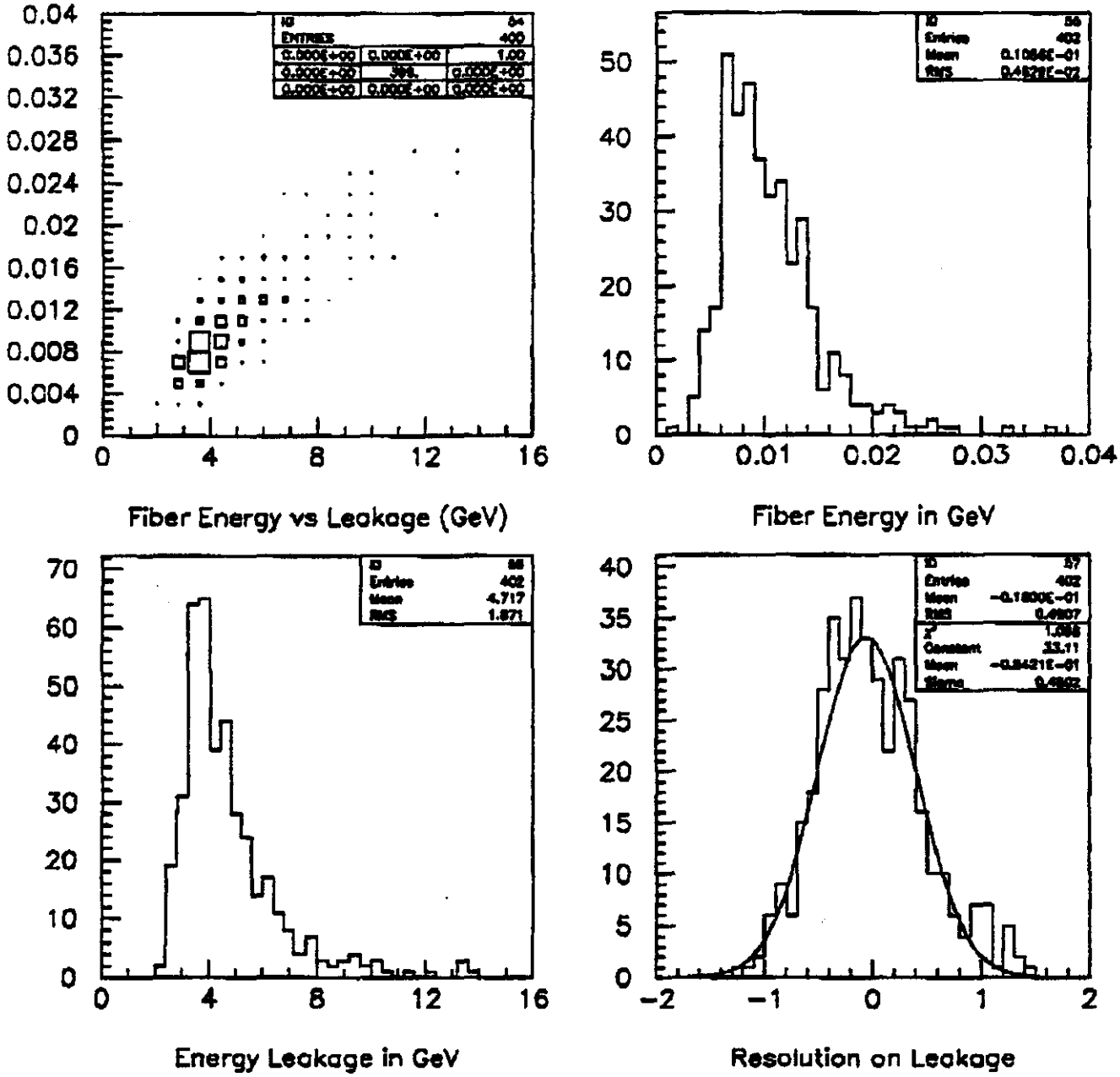

Figure 16
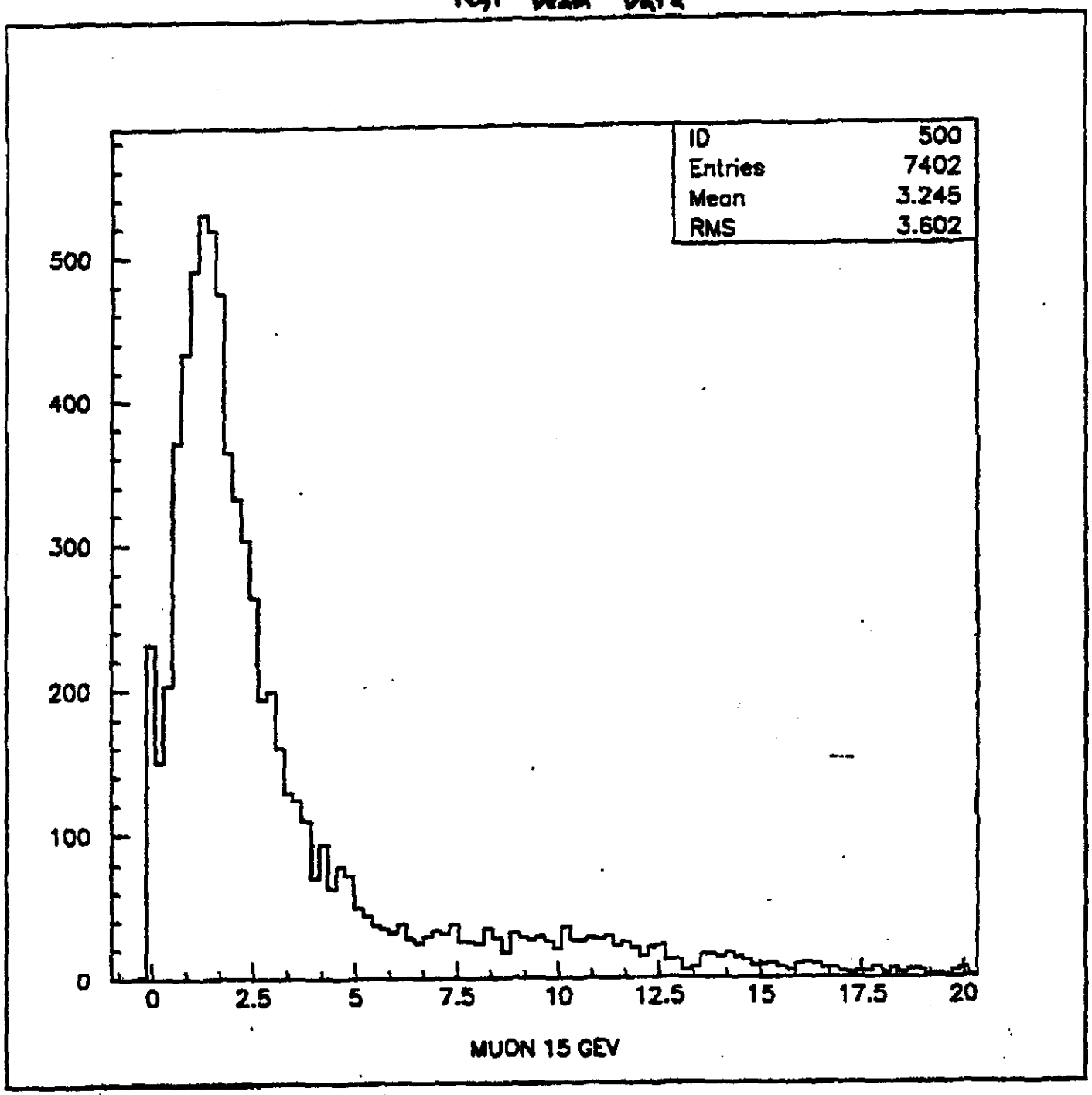
Test Beam Data